Recovering Quantum Correlations in Optical Lattices from Interaction Quenches

Marek Gluza[1,*] and Jens Eisert[1,2,†]
[1]Dahlem Center for Complex Quantum Systems, Freie Universität Berlin, 14195 Berlin, Germany
[2]Helmholtz-Zentrum Berlin für Materialien und Energie, 14109 Berlin, Germany

(Received 7 July 2020; revised 29 March 2021; accepted 13 July 2021; published 24 August 2021)

Quantum simulations with ultracold atoms in optical lattices open up an exciting path toward understanding strongly interacting quantum systems. Atom gas microscopes are crucial for this as they offer single-site density resolution, unparalleled in other quantum many-body systems. However, currently a direct measurement of local coherent currents is out of reach. In this Letter, we show how to achieve that by measuring densities that are altered in response to quenches to noninteracting dynamics, e.g., after tilting the optical lattice. For this, we establish a data analysis method solving the closed set of equations relating tunneling currents and atom number dynamics, allowing us to reliably recover the full covariance matrix, including off-diagonal terms representing coherent currents. The signal processing builds upon semidefinite optimization, providing bona fide covariance matrices optimally matching the observed data. We demonstrate how the obtained information about noncommuting observables allows one to quantify entanglement at finite temperature, which opens up the possibility to study quantum correlations in quantum simulations going beyond classical capabilities.

DOI: 10.1103/PhysRevLett.127.090503

Quantum simulation experiments with ultracold atoms [1] have led to numerous insights into the physics of strongly correlated quantum systems, both in static [2–5] and in dynamical [6–14] regimes. It is fair to say that there has been steady progress toward realizing the ambitious long-term goals set for quantum simulators [15]. Among them, the quest for understanding the precise mechanism underlying the physics of high-T_c superconductors may take a particularly important role, driving forward significant experimental progress on quantum simulations with fermionic systems [16–23]. In this line of research, achieving sufficiently cold temperatures is key and, recently, exciting progress has been reported, signified by an observation of very large antiferromagnets [16] with substantial evidence of string patterns [24]. Thanks to advances toward alleviating this particular bottleneck [25], it may in turn become a make or break issue to develop diagnostic tools regarding genuine quantum correlations in such systems. Specifically, one can anticipate that not only methods for identifying the presence of entanglement will be needed, which can be done via entanglement witnessing, but it will be instrumental to have ways of unambiguously answering the overall physical question of how much entanglement is there in a given quantum many-body system at finite temperature. Tools making this precise, providing certification in this sense [26], should then make it possible to understand the role of quantum mechanical effects on the conductance of systems that have so far evaded modeling using numerical calculations.

In this Letter, we set out to present diagnostic tools capable of tackling exactly these questions. They are based on information that is feasibly available via the so-called "atom gas microscope" [27–29]. Once this innovation had arrived, it allowed one to observe string-order [3–5,16], time-dependent features of ordered [2,6–9,13,30] and disordered models [31]. It should be stressed that these observations would have been much more limited without the atom gas microscope, say, using just time-of-flight-type measurements. The atom microscope has a strong limitation, however, as at any given time it provides information only about the local atom density, which can be captured in terms of commuting operators in a quantum mechanical model. Because of that—possibly surprisingly—exploring quantum correlations in optical lattices is by far not straightforward.

In order to access expectation values of a set of noncommuting observables, one must include some additional operations besides state preparation and direct measurements. Tomographic schemes employing measurements along a single quantization axis in conjunction with Bloch sphere rotations constitute the simplest example. In optical lattices, a sophisticated interference protocol [7] has been demonstrated to reveal entanglement, but it is applicable to only small systems (see also Ref. [32]). Exploiting known time evolution in conjunction with feasible measurements in recovery protocols in a general sense has been explored previously in Refs. [33–47].

As we will show here, observing the density at various times after an interaction quench enables new insights: It allows one to recover expectation values of noncommuting observables and quantify entanglement at finite temperature. This can give clues as to *why* a given system has a

particular value of conductivity and what are the microscopic mechanisms at play in the quantum system studied. Put differently, understanding quantum correlations can allow for physical insights beyond the specific values of system parameters measured by linear response. Linear-response measurements can be done both in quantum simulators and in materials. Concerning the latter, it has been possible to realize superconducting states at very high temperature. If this will be done in optical lattices, then by our method or its possible extensions it will be possible to investigate the role of coherent quantum mechanical effects in the system. This is typically not possible in materials and, in fact, access to sophisticated quantum observables can become one of the most important strengths of quantum simulations in optical lattices [15].

Setting.—The physical setting we have in mind is that of fermionic atoms in optical lattices [19,20]. That said, the technique carries over with little modification to any system in which excitation measurements and noninteracting dynamics are accessible. The discussion focuses on systems in one spatial dimension, but it should be clear that similar ideas carry over to higher-dimensional lattices. It is also worth pointing out that, to an extent, similar ideas have already proven highly useful and experimentally feasible in continuous quantum field settings provided by cold bosonic atoms trapped on an atom chip [33]. Notationwise, we denote fermionic annihilation operators associated with some degree of freedom at lattice site x by $\hat{f}_x$. We put a focus on fermionic systems here, but stress that the same machinery works similarly for bosons as well. The annihilation operators obey the canonical anticommutation relations $\{\hat{f}_x, \hat{f}_y^\dagger\} = \hat{f}_x\hat{f}_y^\dagger + \hat{f}_y^\dagger\hat{f}_x = \delta_{x,y}$. The covariance matrix Γ of a state $\hat{\varrho}$ is defined as the collection of second moments given by

$$\Gamma_{x,y} = \langle \hat{f}_x^\dagger \hat{f}_y \rangle_{\hat{\varrho}} := \mathrm{tr}[\hat{f}_x^\dagger \hat{f}_y \hat{\varrho}]. \tag{1}$$

This matrix is, in general, a complex matrix $\Gamma \in \mathbb{C}^{L\times L}$, with L being the system size [48]. Additionally, we have $\Gamma = \Gamma^\dagger$ which means that it can be unitarily diagonalized by a Bogoliubov transformation of the type

$$\hat{p}_k = \sum_{x=1}^{L} U_{k,x}^* \hat{f}_x, \tag{2}$$

such that $\tilde{\Gamma} = U\Gamma U^\dagger$ with $\tilde{\Gamma}_{k,k'} = \langle \hat{p}_k^\dagger \hat{p}_{k'} \rangle_{\hat{\varrho}}$ being diagonal. Noting that $\hat{n}_k = \hat{p}_k^\dagger \hat{p}_k$ are the number operators of the eigenmodes $\hat{p}_k$, we have that $\tilde{\Gamma} = \mathrm{diag}(\lambda)$ has eigenvalues $0 \le \lambda_k \le 1$ by the Pauli principle. It is useful to write $A \succeq B$ if $A - B$ is a matrix with a non-negative spectrum that yields

$$0 \preccurlyeq \Gamma \preccurlyeq \mathbb{1}. \tag{3}$$

This is a convex constraint that will be included in our reconstructions using semidefinite programming methods [49]. Because of statistical noise, a direct estimate $\Gamma^{(\mathrm{est})}$ of a covariance matrix Γ may not fulfill this constraint, but the recovery procedure should find a physical covariance matrix; hence, taking into account Eq. (3) aids the reliability of the method.

A noninteracting fermionic (free) evolution conserving the particle number is generated by quadratic Hamiltonians

$$\hat{H}(h) = \sum_{x,y=1}^{L} h_{x,y} \hat{f}_x^\dagger \hat{f}_y, \tag{4}$$

where $h = h^\dagger \in \mathbb{C}^{L\times L}$ is the coupling matrix. Most importantly, nearest neighbor hopping (NN) on a line is captured by

$$\hat{H}_{\mathrm{NN}} = \sum_{x=1}^{L-1} \hat{f}_x^\dagger \hat{f}_{x+1} + \mathrm{H.c.}, \tag{5}$$

where we use natural units in terms of the tunneling time throughout the Letter. The Heisenberg evolution of mode operators reads

$$\hat{f}_x(t) = e^{it\hat{H}(h)} \hat{f}_x e^{-it\hat{H}(h)} = \sum_{y=1}^{L} G_{x,y}^*(t) \hat{f}_y, \tag{6}$$

where $G^*(t) = e^{-ith}$ is the propagator matrix, which can be computed efficiently in the system size L. Using Eq. (6) we see that the covariance matrix at time t is

$$\Gamma(t) = G(t)\Gamma(0)G(t)^\dagger. \tag{7}$$

The geometry of the lattice is encoded in the propagator G and by Eq. (7) is imprinted in the correlations. Our recovery method can be formulated independent of specifics of the lattice geometry. However, for clarity only, we shall apply it to the setting of most immediate practical interest, namely, for a chain with open boundary conditions (5).

Tomographic readout from interaction quenches.—The core idea for reconstructing the covariance matrix Γ is the following protocol. The first step is to prepare the state of interest,

$$\text{(a) prepare a fermionic state } \hat{\varrho}. \tag{8}$$

Indeed, we do not have to know anything about how the state is prepared precisely, specifically, whether during the preparation there are nontrivial interactions between the particles or not. The preparation provides a density matrix and we would like to reconstruct the second moments Γ of the possibly non-Gaussian state $\hat{\varrho}$. In the second step, the task is

(b) quench to a free Hamiltonian $\hat{H}(h_{\text{quench}})$. (9)

The ensuing coherent evolution should mix the information about the currents into the occupation numbers dynamics. This quench should be rapid in terms of the tunneling times (which, in practice, means for ultracold atomic experiments that one resorts to narrow Feshbach resonances), but does not have to be perfect. Finally, using the atom microscope, assess the occupation numbers $\hat{N}_x = \hat{f}_x^\dagger \hat{f}_x$

$$\text{(c) measure } N_x(t) \coloneqq \langle \hat{N}_x \rangle_{\hat{\varrho}(t)}. \tag{10}$$

The complete tomographic protocol consists of performing the steps (a)–(c) for times $t = t_1, t_2, \ldots, t_K$, which can be chosen to be equidistant.

This prescription is at this point kept general on purpose, as it can be implemented in various setups and, accordingly, various quench Hamiltonians $\hat{H}(h_{\text{quench}})$ are possible. In this Letter, we show that a suitable such choice is

$$\hat{H}(h_{\text{quench}}) = \hat{H}_{\text{NN}} + \sum_x \mu_x \hat{N}_x, \tag{11}$$

where $\mu_x = x$ represents a gradient of the chemical potential. Additional simulations, presented in the Supplemental Material [50], demonstrate that quenches into a doubled-up lattice or involving artificial magnetic fields can be also advantageous, in settings where this is feasible. This works because in (c) we are acquiring information about currents due to the equation

$$N_x(t) = \Gamma_{x,x}(t) = \sum_{y,y'=1}^{L} G_{x,y}(t) G^*_{x,y'}(t) \Gamma_{y,y'}(0). \tag{12}$$

We find that, generically, the right-hand side will depend on the off-diagonal matrix elements in the initial covariance matrix. The reconstruction procedure makes use of the reversed direction of this equality and can be intuited as harvesting information about the currents from the response of the particle number dynamics following the quench.

The reconstruction is based on an algorithm that, in a nutshell, takes a guess for the covariance matrix Γ', evolves forward to the times t_i where the particle number data has been measured, and checks whether the extrapolated distribution of the particles $N_x(t_i;\Gamma') = \Gamma'_{x,x}(t_i)$ reproduces the data $N_x(t_i;\Gamma') \approx N_x(t_i)$. In the next step, an improved guess Γ'' is obtained, such that the new observables $N_x(t_i;\Gamma'')$ are closer to the data

$$|N_x(t_i;\Gamma'') - N_x(t_i)| \leq |N_x(t_i;\Gamma') - N_x(t_i)|. \tag{13}$$

By iterating this, the algorithm solves the following optimization task. We collect all measured data into a vector b and define a linear map $\mathcal{A}$, which from an input covariance matrix Γ' produces the respective occupation numbers $N_x(t_i;\Gamma')$ in the same ordering as in b. The reconstruction $\Gamma^{(\text{Rec})}$ is the optimal solution to the optimization problem

$$\min_{0 \leqslant \Gamma' \leqslant \mathbb{1}} \|\mathcal{A}(\Gamma') - b\|_2. \tag{14}$$

The cost function is the 2-norm, so we need to perform a least-square recovery problem with a positivity constraint [49]. Convexity of the problem guarantees an efficient convergence to a globally optimal solution with a polynomial runtime in the system size L and desired accuracy $\epsilon > 0$ [49] and, in practice, takes a few seconds for $L \approx 40$.

To exemplify the functioning of the method, we consider thermal states $\hat{\varrho}_\beta = e^{-\beta \hat{H}_{\text{NN}}}/Z_\beta$, where Z_β is the partition function, $\beta > 0$ is the inverse temperature, and $\Gamma^{(\beta)}$ is the corresponding covariance matrix. The results of the numerical reconstruction [68] are presented in Fig. 1. The particle number measurement need not be perfect and Fig. 1 discusses reconstructions that include statistical noise from necessarily finite numbers of measurements.

In step (a), additional assumptions can be included, such as translation invariance in the initial state or a finite

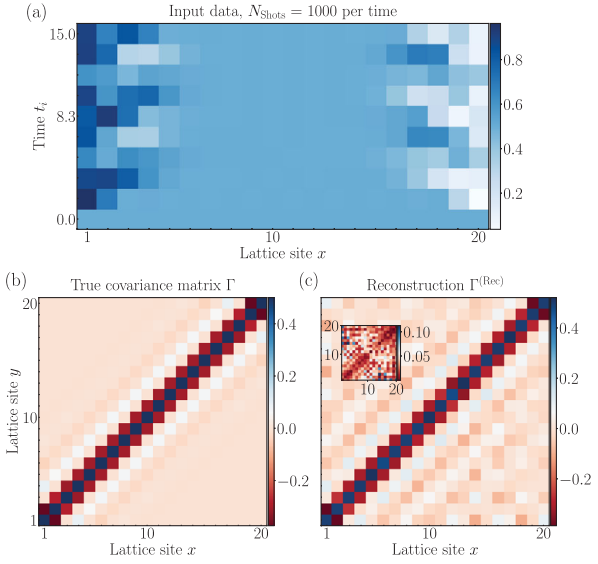

FIG. 1. Tomographic reconstruction. (a) Input data for the reconstruction based on out-of-equilibrium data of local particle numbers $N_x(t_i)$ measured at $K = 10$ equidistant times after the quench to nearest-neighbor hopping in the tilted lattice. We model statistical fluctuations by sampling occupation numbers $\mathcal{N}_{\text{shots}} = 10^3$ times for each t_i and estimating $N_x(t_i)$ via the empirical mean. (b) The input data have been obtained by evolving a thermal covariance of $\hat{H}_{\text{NN}}$ with inverse temperature $\beta = 3$ such that there are relatively large currents to be recovered. (c) Results of the reconstruction $\Gamma^{(\text{Rec})}$. The extent of deviations shown in the inset is $\max |\Gamma_{x,y} - \Gamma^{(\text{Rec})}_{x,y}| \approx 0.1$ and is explained by the fact that among the data some $N_x(t_i)$ can fluctuate statistically by 2 or 3 standard deviations.

correlation length. The quench is motivated by existing control functionalities; see, e.g., Ref. [69] for an experimental study showcasing a superb degree of coherence in the system when tilting the optical lattice. We remark that other quenches that lead to nontrivial dynamics (the covariance matrix is not a steady state of the quench Hamiltonian) can be considered. The reconstruction code [68] does not depend on the quench Hamiltonian being nearest neighbor or whether there is a trap present, so other variants are possible; see the Supplemental Material [50]. If the couplings h are real, then the tomography reconstructs only the real part of the currents. This is enough for thermal states of quadratic Hamiltonians with no magnetic fields; see [50] for reconstructions in their presence. Finally, note that similar ideas have successfully been applied in an atom chip experiment for a continuum system [33] where some unknown stray interactions have been present [70], but have been negligible in short time windows.

Quantum simulation studies of low-temperature systems in presence of Hubbard interactions with strength U are of particular interest. Our method can be used to measure the second moments of interacting states by switching off $U \mapsto 0$ as fast as possible, e.g., by choosing narrow Feshbach resonances (see the Supplemental Material [50] for comparisons of ramps of varying duration compared to the tunneling time). Crucially though, it follows directly from the Lieb-Robinson bound [71] that, even if the quench has a finite duration, only the local correlations will be affected but, e.g., the method can uncover the presence of correlations spanning far-away sites. If the quench has a negligible duration compared to the relevant timescales in the system, then even local correlations will be faithfully reconstructed, implying the possibility of measuring also the kinetic energy in addition to the Hubbard interaction term that can be measured with the atom microscope. Our method does not assume translation invariance or thermality of the unknown state, which are the cornerstones but also limitations of existing methods [72–79] and hence can pave the way toward reading out the results of variational quantum simulations [80] in optical lattices for systems with a complicated connectivity graph.

Quantitatively estimating fermionic mode entanglement.—Let us now show how to analyze the second moments Γ of a possibly interacting or nonequilibrium state to lower bound the so-called entanglement cost [60,61]. This statement is particularly appealing, as it goes beyond merely showing that there is entanglement present, but also provides an answer to the question of "how much" entanglement there is in the system [81–84]. The entanglement cost E_C quantifies mixed-state entanglement [60,61], as it is the asymptotic rate at which maximally entangled pairs must be used for the creation of a given state $\hat{\varrho}$ using local operations with classical communication (LOCC). E_C is broadly studied in quantum information theory, but is not easy to access in practice and, therefore, especially in the context of experiments, lower bounds by means of practically measurable quantities are needed.

We consider $\hat{\varrho}$ to describe a bipartite system $A \cup B$, e.g., some number of sites in an optical lattice, and will explain how to lower bound $E_C(\hat{\varrho})$. First, if the asymptotically optimal creation of the state $\hat{\varrho}$ via LOCC necessitates maximally entangled pairs at rate $E_C(\hat{\varrho})$, then it could be that even more entangled pairs are needed for a system consisting of fermionic particles. Indeed, any physical operation in this case is subject to the fermionic parity and total number superselection rules (SSRs) [56,57] which further restrict LOCC. However, in Ref. [85], it has been shown that the asymptotic rates do not change, i.e., $E_C^{\mathrm{SSR}}(\hat{\varrho}) = E_C(\hat{\varrho})$ (see the Supplemental Material [50]). Second, we use that the entanglement cost is lower bounded by distillable entanglement E_D [60,61]

$$E_C(\hat{\varrho}) \geq E_D(\hat{\varrho}). \tag{15}$$

In fact, in our discussion, we can equally well also refer to the distillable entanglement. Third, the distillable entanglement is lower bounded by virtue of the hashing bound [86]

$$E_D(\hat{\varrho}) \geq S(\hat{\varrho}_A) - S(\hat{\varrho}), \tag{16}$$

where for any state $\hat{\sigma}$ the von Neumann entropy is $S(\hat{\sigma}) = -\mathrm{tr}[\hat{\sigma}\log_2(\hat{\sigma})]$ and the subscript in $\hat{\varrho}_A$ indicates the reduction to subsystem A. Finally, the right-hand side can be lower bounded by the same expression, but now in terms of Gaussian entropies. Specifically, let us denote by $S^{(\Gamma)} = S(\hat{\varrho}_\Gamma)$ the von Neumann entropy of a fermionic Gaussian state $\hat{\varrho}_\Gamma$ with the same second moments Γ as $\hat{\varrho}$. As shown in Refs. [87,88], we have

$$S(\hat{\varrho}_A) - S(\hat{\varrho}) \geq S^{(\Gamma_A)} - S^{(\Gamma)} \coloneqq E_G(\Gamma). \tag{17}$$

The Gaussian entropy $S^{(\Gamma)}$ can be easily computed from the recovered covariance matrix $\Gamma^{(\mathrm{Rec})}$; see the Supplemental Material [50] for details. Summarizing, for any bipartite state $\hat{\varrho}$ whose second moments Γ one can measure using our method, we have found a lower bound to the entanglement cost $E_G(\Gamma) \leq E_C(\hat{\varrho})$.

Entanglement cost at finite temperatures.—In what follows, we discuss the application of the witness to again assess thermal states of $\hat{H}_{\mathrm{NN}}$. As detailed in the Supplemental Material [50], without increasing E_C we can perform a local unitary Bogoliubov transformation in subsystems A and B individually. In Fig. 2(a) we show the covariance matrix for $\beta = 3$ after such a local transformation showing that essentially two modes are nontrivially correlated. In Fig. 2(b) we depict the entanglement cost lower bound $E_G(\beta) \coloneqq E_G(\Gamma^{(\beta)})$ as a function of inverse temperature. We select either one or two modes in each subsystem and find a nontrivial lower bound $E_G(\beta) > 0$ for sufficiently low temperatures. Choosing one mode gives a

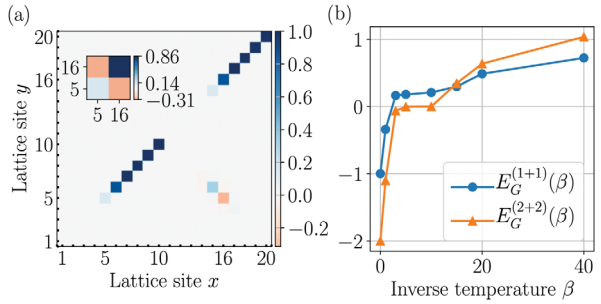

FIG. 2. Entanglement cost at finite temperature. (a) The covariance matrix $\Gamma^{(D)} = U_D \Gamma^{(\beta)} U_D^\dagger$ for the inverse temperature $\beta = 3$ after a suitable local transformation $U_D = U_A \oplus U_B$ preserving the entanglement. The inset shows the submatrix of the covariance matrix reflecting one mode in subsystem A and one in B. (b) This figure shows how the lower bound for the entanglement depends on whether it is applied on one or two modes in systems A and B each. Selecting merely one mode each provides a positive entanglement cost for relatively large temperatures ($E_G^{(1+1)}$), while two modes are better suited to detect entanglement at low temperatures [$E_G^{(2+2)}(\beta)$].

nontrivial lower bound for higher temperatures than for two modes because the total entropy in the latter case tends to be larger at high temperature. In contrast, at extremely low temperatures, the one mode lower bound saturates at its maximum value $E_G^{(1+1)}(\beta) \leq 1$, while the two mode witness indicates that the entanglement cost of preparing $\hat{\varrho}_\beta$ is asymptotically larger than that of one maximally entangled pair. Going beyond the Gaussian case, note that the second moments of low-temperature states will vary continuously with the strength of the many-body interaction [89]. Thus, we can be confident that a nontrivial E_C lower bound will be obtained for sufficiently weak interactions and low temperatures. Such states, e.g., in two spacial dimensions, become difficult to treat numerically in practice; however, our reconstruction and entanglement quantification methods remain applicable for quantum simulations.

Outlook.—In this Letter, we have shown how to recover the full covariance matrix of quantum states in optical lattices by unifying atom microscope measurements with suitable quenches and performing efficient reconstructions using semidefinite programming. The method introduced here is reliable and versatile as it does not depend on the geometry of the quench: Other ways of inducing visible particle number dynamics specific to a given setup can also be considered and some other ideas are discussed in the Supplemental Material [50]. The prospect of advancing our data analysis by making use of recent theoretical ideas, such as shadow estimation [45] or random operations that can be efficiently classically backtracked [34,90], should also be noted. Building on the accessibility of full covariance matrices, including coherent currents, we have exploited an entropic witness that allows one to lower bound the entanglement cost and the distillable entanglement. This is a quantitative measure of entanglement implying a substantially stronger statement than merely showing its presence. We have shown that our witness can give nontrivial values at finite temperatures. This will remain true also for weak interactions, as second moments should vary continuously in the strength of interactions. We hence have established a method to recover and quantify quantum correlations in optical lattice quantum simulations that is applicable even in regimes where numerical calculations cease being practical.

The numerical code used in this Letter is freely available at https://github.com/marekgluza/hopping_tomography and includes interactive PYTHON notebooks allowing one to reproduce the figures [68].

We thank M. Greiner, C. Gross, P. Preiss, and R. Sweke for stimulating discussions. This work has been supported by the ERC (TAQ), the DFG (CRC 183, FOR 2724, EI 519/7-1), the BMBF (DAQC for analog benchmarking techniques and FermiQP for techniques for readout in cold atomic platforms), and the Templeton Foundation. This work has also received funding from the European Union's Horizon 2020 Research and Innovation Programme under Grant Agreement No. 817482 (PASQuanS).

*marekgluza@zedat.fu-berlin.de
†jense@zedat.fu-berlin.de

[1] I. Bloch, J. Dalibard, and S. Nascimbene, Nat. Phys. **8**, 267 (2012).
[2] M. Greiner, I. Bloch, O. Mandel, T. W. Hänsch, and T. Esslinger, Phys. Rev. Lett. **87**, 160405 (2001).
[3] M. Endres, M. Cheneau, T. Fukuhara, C. Weitenberg, P. Schauss, C. Gross, L. Mazza, M. C. Banuls, L. Pollet, I. Bloch, and S. Kuhr, Science **334**, 200 (2011).
[4] M. E. Tai, A. Lukin, M. Rispoli, R. Schittko, T. Menke, D. Borgnia, P. M. Preiss, F. Grusdt, A. M. Kaufman, and M. Greiner, Nature (London) **546**, 519 (2017).
[5] S. Trotzky, L. Pollet, F. Gerbier, U. Schnorrberger, I. Bloch, N. Prokof'ev, B. Svistunov, and M. Troyer, Nat. Phys. **6**, 998 (2010).
[6] S. Trotzky, Y.-A. Chen, A. Flesch, I. P. McCulloch, U. Schollwöck, J. Eisert, and I. Bloch, Nat. Phys. **8**, 325 (2012).
[7] A. M. Kaufman, M. E. Tai, A. Lukin, M. Rispoli, R. Schittko, P. M. Preiss, and M. Greiner, Science **353**, 794 (2016).
[8] S. Braun, M. Friesdorf, S. S. Hodgman, M. Schreiber, J. P. P. Ronzheimer, A. Riera, M. del Rey, I. Bloch, J. Eisert, and U. Schneider, Proc. Natl. Acad. Sci. U.S.A. **112**, 3641 (2015).
[9] J. P. Ronzheimer, M. Schreiber, S. Braun, S. S. Hodgman, S. Langer, I. P. McCulloch, F. Heidrich-Meisner, I. Bloch, and U. Schneider, Phys. Rev. Lett. **110**, 205301 (2013).
[10] S. Hofferberth, I. Lesanovsky, B. Fischer, T. Schumm, and J. Schmiedmayer, Nature (London) **449**, 324 (2007).
[11] M. Gring, M. Kuhnert, T. Langen, T. Kitagawa, B. Rauer, M. Schreitl, I. Mazets, D. A. Smith, E. Demler, and J. Schmiedmayer, Science **337**, 1318 (2012).

[12] T. Langen, S. Erne, R. Geiger, B. Rauer, T. Schweigler, M. Kuhnert, W. Rohringer, I. E. Mazets, T. Gasenzer, and J. Schmiedmayer, Science **348**, 207 (2015).

[13] M. Cheneau, P. Barmettler, D. Poletti, M. Endres, P. Schauss, T. Fukuhara, C. Gross, I. Bloch, C. Kollath, and S. Kuhr, Nature (London) **481**, 484 (2012).

[14] T. Schweigler, V. Kasper, S. Erne, I. E. Mazets, B. Rauer, F. Cataldini, T. Langen, T. Gasenzer, J. Berges, and J. Schmiedmayer, Nature (London) **545**, 323 (2017).

[15] A. Acin, I. Bloch, H. Buhrman, T. Calarco, C. Eichler, J. Eisert, D. Esteve, N. Gisin, S. J. Glaser, F. Jelezko, S. Kuhr, M. Lewenstein, M. F. Riedel, P. O. Schmidt, R. Thew, A. Wallraff, I. Walmsley, and F. K. Wilhelm, New J. Phys. **20**, 080201 (2018).

[16] A. Mazurenko, C. S. Chiu, G. Ji, M. F. Parsons, M. Kanasz-Nagy, R. Schmidt, F. G. E. Demler, Greif, and M. Greiner, Nature (London) **545**, 462 (2017).

[17] M. Köhl, H. Moritz, T. Stöferle, K. Günter, and T. Esslinger, Phys. Rev. Lett. **94**, 080403 (2005).

[18] T. Esslinger, Annu. Rev. Condens. Matter Phys. **1**, 129 (2010).

[19] U. Schneider, L. Hackermüller, J. P. Ronzheimer, S. Will, T. B. S. Braun, I. Bloch, E. Demler, S. Mandt, D. Rasch, and A. Rosch, Nat. Phys. **8**, 213 (2012).

[20] T. Rom, T. Best, D. van Oosten, U. Schneider, S. Foelling, B. Paredes, and I. Bloch, Nature (London) **444**, 733 (2006).

[21] C. S. Chiu, G. Ji, A. Mazurenko, D. Greif, and M. Greiner, Phys. Rev. Lett. **120**, 243201 (2018).

[22] A. Behrle, T. Harrison, J. Kombe, K. Gao, M. Link, J.-S. Bernier, C. Kollath, and M. Köhl, Nat. Phys. **14**, 781 (2018).

[23] K. Viebahn, M. Sbroscia, E. Carter, J.-C. Yu, and U. Schneider, Phys. Rev. Lett. **122**, 110404 (2019).

[24] C. S. Chiu, G. Ji, A. Bohrdt, M. Xu, M. Knap, E. Demler, F. Grusdt, M. Greiner, and D. Greif, Science **365**, 251 (2019).

[25] B. Yang, H. Sun, C.-J. Huang, H.-Y. Wang, Y. Deng, H.-N. Dai, Z.-S. Yuan, and J.-W. Pan, Science **369**, 550 (2020).

[26] J. Eisert, D. Hangleiter, N. Walk, I. Roth, D. Markham, R. Parekh, U. Chabaud, and E. Kashefi, Nat. Rev. Phys. **2**, 382 (2020).

[27] J. F. Sherson, C. Weitenberg, M. Endres, M. Cheneau, I. Bloch, and S. Kuhr, Nature (London) **467**, 68 (2010).

[28] W. S. Bakr, A. Peng, M. E. Tai, R. Ma, J. Simon, J. I. Gillen, S. Fölling, L. Pollet, and M. Greiner, Science **329**, 547 (2010).

[29] C. Weitenberg, M. Endres, J. F. Sherson, M. Cheneau, P. Schauß, T. Fukuhara, I. Bloch, and S. Kuhr, Nature (London) **471**, 319 (2011).

[30] J. Eisert, M. Friesdorf, and C. Gogolin, Nat. Phys. **11**, 124 (2015).

[31] M. Schreiber, S. S. Hodgman, P. Bordia, H. P. Lüschen, M. H. Fischer, R. Vosk, E. Altman, U. Schneider, and I. Bloch, Science **349**, 842 (2015).

[32] A. Bergschneider, V. M. Klinkhamer, J. H. Becher, R. Klemt, L. Palm, G. Zürn, S. Jochim, and P. M. Preiss, Nat. Phys. **15**, 640 (2019).

[33] M. Gluza, T. Schweigler, B. Rauer, C. Krumnow, J. Schmiedmayer, and J. Eisert, Commu. Phys. **3**, 12 (2020).

[34] M. Ohliger, V. Nesme, and J. Eisert, New J. Phys. **15**, 015024 (2013).

[35] S. T. Merkel, C. A. Riofrío, S. T. Flammia, and I. H. Deutsch, Phys. Rev. A **81**, 032126 (2010).

[36] A. Elben, B. Vermersch, M. Dalmonte, J. I. Cirac, and P. Zoller, Phys. Rev. Lett. **120**, 050406 (2018).

[37] P. Hauke, M. Lewenstein, and A. Eckardt, Phys. Rev. Lett. **113**, 045303 (2014).

[38] L. A. Pena Ardila, M. Heyl, and A. Eckardt, Phys. Rev. Lett. **121**, 260401 (2018).

[39] T. Qin, A. Schnell, K. Sengstock, C. Weitenberg, A. Eckardt, and W. Hofstetter, Phys. Rev. A **98**, 033601 (2018).

[40] M. Tarnowski, F. N. Ünal, N. Fläschner, B. S. Rem, A. Eckardt, K. Sengstock, and C. Weitenberg, Nat. Commun. **10**, 1728 (2019).

[41] S. Keßler and F. Marquardt, Phys. Rev. A **89**, 061601(R) (2014).

[42] K. Loida, J.-S. Bernier, R. Citro, E. Orignac, and C. Kollath, Phys. Rev. A **98**, 033605 (2018).

[43] M. Atala, M. Aidelsburger, M. Lohse, J. T. Barreiro, B. Paredes, and I. Bloch, Nat. Phys. **10**, 588 (2014).

[44] C. Schweizer, M. Lohse, R. Citro, and I. Bloch, Phys. Rev. Lett. **117**, 170405 (2016).

[45] H.-Y. Huang, R. Kueng, and J. Preskill, Nat. Phys. **16**, 1050 (2020).

[46] B. Bergh and M. Gärttner, Phys. Rev. A **103**, 052412 (2021).

[47] B. Bergh and M. Gärttner, Phys. Rev. Lett. **126**, 190503 (2021).

[48] If it was possible to directly measure currents, then one would measure $\mathrm{Re}[\Gamma_{x,y}] = \frac{1}{2}\langle \hat{f}_x^\dagger \hat{f}_y + \hat{f}_y^\dagger \hat{f}_x \rangle_{\hat{\varrho}}$ and $\mathrm{Im}[\Gamma_{x,y}] = -(i/2)\langle \hat{f}_x^\dagger \hat{f}_y - \hat{f}_y^\dagger \hat{f}_x \rangle_{\hat{\varrho}}$ (the latter vanishes oftentimes given appropriate symmetries in the system).

[49] S. Boyd and L. Vandenberghe, Convex Optimization (Cambridge University Press, Cambridge, England, 2016), https://www.cambridge.org/gb/academic/subjects/statistics-probability/optimization-or-and-risk/convex-optimization?format=HB.

[50] See the Supplemental Material at http://link.aps.org/supplemental/10.1103/PhysRevLett.127.090503, which contains Refs. [6,26,51–67], for additional details concerning reconstructions of various initial conditions, including thermal Hubbard and Anderson insulator chains, ideas for other protocols and for experimental benchmarking of the method, and extended discussion of fermionic mode entanglement together with details on the evaluation of the witness.

[51] M. B. Hastings and T. Koma, Commun. Math. Phys. **265**, 781 (2006).

[52] S. Bera, H. Schomerus, F. Heidrich-Meisner, and J. H. Bardarson, Phys. Rev. Lett. **115**, 046603 (2015).

[53] M. Gluza, M. Kliesch, J. Eisert, and L. Aolita, Phys. Rev. Lett. **120**, 190501 (2018).

[54] F. Arute, K. Arya, R. Babbush, D. Bacon, J. C. Bardin, R. Barends, S. Boixo, M. Broughton, B. B. Buckley, D. A. Buell *et al.*, arXiv:2004.04174.

[55] S. T. Flammia and Y.-K. Liu, Phys. Rev. Lett. **106**, 230501 (2011).

[56] J. Earman, Erkenntnis **69**, 377 (2008).

[57] G. C. Wick, A. S. Wightman, and E. P. Wigner, Phys. Rev. **88**, 101 (1952).

[58] M. A. Nielsen, Phys. Rev. Lett. **83**, 436 (1999).

[59] J. Eisert and M. Cramer, Phys. Rev. A **72**, 042112 (2005).

[60] C. H. Bennett, H. J. Bernstein, S. Popescu, and B. Schumacher, Phys. Rev. A **53**, 2046 (1996).
[61] R. Horodecki, P. Horodecki, M. Horodecki, and K. Horodecki, Rev. Mod. Phys. **81**, 865 (2009).
[62] N. Schuch, F. Verstraete, and J. I. Cirac, Phys. Rev. A **70**, 042310 (2004).
[63] M. Gluza, C. Krumnow, M. Friesdorf, C. Gogolin, and J. Eisert, Phys. Rev. Lett. **117**, 190602 (2016).
[64] M. M. Wolf, Phys. Rev. Lett. **96**, 010404 (2006).
[65] I. Peschel, J. Stat. Mech. (2004) P12005.
[66] J. Eisert, V. Eisler, and Z. Zimboras, Phys. Rev. B **97**, 165123 (2018).
[67] G. Roósz, Z. Zimborás, and R. Juhász, Phys. Rev. B **102**, 064204 (2020).
[68] M. Gluza, Version v1, GitHub repository HoppingTomography (2021), https://doi.org/10.5281/zenodo.5163265.
[69] P. M. Preiss, R. Ma, M. E. Tai, A. Lukin, M. Rispoli, P. Zupancic, Y. Lahini, R. Islam, and M. Greiner, Science **347**, 1229 (2015).
[70] B. Rauer, S. Erne, T. Schweigler, F. Cataldini, M. Tajik, and J. Schmiedmayer, Science **360**, 307 (2018).
[71] E. H. Lieb and D. W. Robinson, Commun. Math. Phys. **28**, 251 (1972).
[72] T. Hartke, B. Oreg, N. Jia, and M. Zwierlein, Phys. Rev. Lett. **125**, 113601 (2020).
[73] M. A. Nichols, L. W. Cheuk, M. Okan, T. R. Hartke, E. Mendez, T. Senthil, E. Khatami, H. Zhang, and M. W. Zwierlein, Science **363**, 383 (2019).
[74] P. T. Brown, D. Mitra, E. Guardado-Sanchez, R. Nourafkan, A. Reymbaut, C.-D. Hébert, S. Bergeron, A.-M. S. Tremblay, J. Kokalj, D. A. Huse, P. Schauß, and W. S. Bakr, Science **363**, 379 (2019).
[75] Y. Takasu, T. Yagami, H. Asaka, Y. Fukushima, K. Nagao, S. Goto, I. Danshita, and Y. Takahashi, Sci. Adv. **6**, eaba9255 (2020).
[76] Y. Nakamura, Y. Takasu, J. Kobayashi, H. Asaka, Y. Fukushima, K. Inaba, M. Yamashita, and Y. Takahashi, Phys. Rev. A **99**, 033609 (2019).
[77] E. Cocchi, L. A. Miller, J. H. Drewes, C. F. Chan, D. Pertot, F. Brennecke, and M. Köhl, Phys. Rev. X **7**, 031025 (2017).
[78] C. F. Chan, M. Gall, N. Wurz, and M. Köhl, Phys. Rev. Research **2**, 023210 (2020).
[79] E. Guardado-Sanchez, A. Morningstar, B. M. Spar, P. T. Brown, D. A. Huse, and W. S. Bakr, Phys. Rev. X **10**, 011042 (2020).
[80] C. Kokail, C. Maier, R. van Bijnen, T. Brydges, M. K. Joshi, P. Jurcevic, C. A. Muschik, P. Silvi, R. Blatt, C. F. Roos *et al.*, Nature (London) **569**, 355 (2019).
[81] J. Eisert, F. G. Brandao, and K. M. Audenaert, New J. Phys. **9**, 46 (2007).
[82] K. M. R. Audenaert and M. B. Plenio, New J. Phys. **8**, 266 (2006).
[83] O. Gühne, M. Reimpell, and R. F. Werner, Phys. Rev. Lett. **98**, 110502 (2007).
[84] M. Cramer, A. Bernard, N. Fabbri, L. Fallani, C. Fort, S. Rosi, F. Caruso, M. Inguscio, and M. Plenio, Nat. Commun. **4**, 2161 (2013).
[85] N. Schuch, F. Verstraete, and J. I. Cirac, Phys. Rev. A **70**, 042310 (2004).
[86] I. Devetak and A. Winter, Proc. R. Soc. A **461**, 207 (2005).
[87] F. Pastawski, J. Eisert, and H. Wilming, Phys. Rev. Lett. **119**, 020501 (2017).
[88] J. Eisert and M. W. Wolf, Gaussian quantum channels, in *Quantum Information with Continuous Variables of Atoms and Light* (Imperial College Press, London, 2007), pp. 23–42.
[89] C. V. Kraus and J. I. Cirac, New J. Phys. **12**, 113004 (2010).
[90] T. Brydges, A. Elben, P. Jurcevic, B. Vermersch, C. Maier, B. P. Lanyon, P. Zoller, R. Blatt, and C. F. Roos, Science **364**, 260 (2019).